Integrative Biology

RSC Publishing

TECHNICAL INNOVATION

View Article Online
View Journal | View Issue

Open Access Article. Published on 17 April 2013. Downloaded on 15/11/2014 00:35:09.

Cite this: *Integr. Biol.*, 2013, **5**, 889

In vivo screening of extracellular matrix components produced under multiple experimental conditions implanted in one animal†

Gustavo A. Higuera,‡*[b] Jeanine A. A. Hendriks,‡[c] Joost van Dalum,[a] Ling Wu,[a] Roka Schotel,[c] Liliana Moreira-Teixeira,[a] Mirella van den Doel,[c] Jeroen C. H. Leijten,[a] Jens Riesle,[c] Marcel Karperien,[a] Clemens A. van Blitterswijk[a] and Lorenzo Moroni[a]

Animal experiments help to progress and ensure safety of an increasing number of novel therapies, drug development and chemicals. Unfortunately, these also lead to major ethical concerns, costs and limited experimental capacity. We foresee a coercion of all these issues by implantation of well systems directly into vertebrate animals. Here, we used rapid prototyping to create wells with biomaterials to create a three-dimensional (3D) well-system that can be used *in vitro* and *in vivo*. First, the well sizes and numbers were adjusted for 3D cell culture and *in vitro* screening of molecules. Then, the functionality of the wells was evaluated *in vivo* under 36 conditions for tissue regeneration involving human mesenchymal stem cells (hMSCs) and bovine primary chondrocytes (bPCs) screened in one animal. Each biocompatible well was controlled to contain μl-size volumes of tissue, which led to tissue penetration from the host and tissue formation under implanted conditions. We quantified both physically and biologically the amounts of extracellular matrix (ECM) components found in each well. Using this new concept the co-culture of hMSCs and bPCs was identified as a positive hit for cartilage tissue repair, which was a comparable result using conventional methods. The *in vivo* screening of candidate conditions opens an entirely new range of experimental possibilities, which significantly abates experimental animal use and increases the pace of discovery of medical treatments.

Received 31st January 2013,
Accepted 5th April 2013

DOI: 10.1039/c3ib40023a

www.rsc.org/ibiology

Insight, innovation, integration

Well-plates and their experimental throughput, as invented by Dr Gyula Takatsy in 1951, are indispensable tools in biological research, where biological data throughput remains solely optimised *in vitro*. Here, we created implantable well-plates to increase the throughput of animal experiments. By creating wells with biocompatible materials, it was possible to evaluate μl-size volumes of tissue *in vitro* and *in vivo* and to obtain quantitative correlations of multiple conditions *vs.* biological markers directly in animal models. This approach embodies a practical strategy to reduce the numbers of experimental animals that rely on analysing tissue biology in units (wells) that can be controlled and compared with other units of real tissue.

Introduction

New biomedical treatments spend years in the preclinical phase due to the inherent difficulties in translating[1,2] *in vitro* results into *in vivo* settings and their subsequent rounds of decisive[3,4] validation in ethically and financially costly animal models. While novel *in vitro* methods[5] have boosted the throughput of data and predictability of treatments in animals, the benefit of *in vitro* models to forecast *in vivo* effects has not been definitely proven.[1,6] For example, novel drug screening methods[7] do not consider physical phenomena typical of three-dimensional (3D) tissues such as molecular diffusion and gradient profiles. In such cases, *in vitro* validation for drug and treatment development depends on gene expression profiles that usually differ from the effects of sharp molecular gradients of the native 3D milieu.

Another approach to replacing animal experiments has seen the rise of promising 3D[8] and micro-fabricated systems[9–13] that try to mimic the cellular environment. These systems capture some of the complexity of the 3D environment; that is, the role of physics in tissue biology.[14] However, most of these fall

[a] *Department of Tissue Regeneration, MIRA Institute, University of Twente, Drienerlolaan 5, Zuidhorst, 7522 NB Enschede, The Netherlands. E-mail: gustavo.higuera@screvo.net; Fax: +31 53489 2150; Tel: +31 53489 3400*
[b] *Screvo Ltd, P.O. Box 217, 7500 AE, Enschede, The Netherlands*
[c] *CellCoTec, Prof. Bronkhorstlaan 10-48, 3723MB Bilthoven, The Netherlands*

† Electronic supplementary information (ESI) available. See DOI: 10.1039/c3ib40023a

‡ Both authors contributed equally.

Open Access Article. Published on 17 April 2013. Downloaded on 15/11/2014 00:35:09.

short of representing real tissue and replacing animal models. Inevitably, millions of animals are bred every year to evaluate the impact of substances and treatments on the environment and human health.

A notable example for optimizing animal experiments has been achieved in evaluating biocompatibility,[15] where 8 biomaterials can be spatio-temporally assessed in one animal through fluorescence imaging. Even though the physiological consequences for implanting multiple conditions (*e.g.* materials, drugs or toxins) in one animal cannot be predicted, and must therefore be investigated, there is a tangible social and economic benefit of increasing the efficiency of experiments directly in animal models.

Here, we integrate methodology in rapid prototyping, 3D cell culture and ECM biology to present *in vivo* screening as a viable strategy for refining animal experiments. To make this possible, we made an implantable well-system that enables screening *in vitro* and directly in an animal model for tissue regeneration. For cell culture, human mesenchymal stem cells (hMSCs) and bovine primary chondrocytes (bPCs) were chosen as cell sources for their extensively studied therapeutic potential. We focus on screening of ECM components as markers of the tissue formation potential of 36 cell conditions in one animal.

Results and discussion

To screen *in vivo*, that is, to implant multiple conditions directly in one animal, conventional platforms and screening materials such as polydimethylsiloxane (PDMS) would not be ideal due to biocompatibility concerns. Therefore, we decided to create a platform made of biomaterials. The versatility of free form fabrication allowed us to manufacture[16] a system of wells with a wide range of materials (Table S1 and Fig. S1, ESI†), where the well, numbers, material and architecture can be defined depending on the implantation site of the animal (Fig. 1). These implantable devices consist of μm^3 to mm^3 size wells organized in column × row arrays.

We then tested the robustness of wells by dispensing specimens that could be manually seeded and that were compatible with standard laboratory equipment (Fig. S2, ESI†) such as an automatic confocal microscope (Fig. S2B, ESI†). In these *in vitro* experiments, the wells were randomly seeded with dyes of different colors (Fig. S2A–E, ESI†) to confirm that there was no cross-contamination between different wells and unbiased readouts. We first used microspheres and fluorescent markers (Fig. S2F, ESI†) to evaluate if compounds with different sizes and fluorescent properties could be quantified in the wells. The intensity of light emitted from poly lactic acid wells containing microspheres revealed that the mean fluorescent intensity (n = 3) significantly decreased with increasing dilution factors (Fig. S2B, ESI†). When the fluorescent markers rhodamine and fluorescein isothiocyanate (FITC) were seeded at different dilutions in photo-sensible resin-made wells (Fig. S2F, ESI†), these also displayed a significant correlation between the dilution factor and mean light intensity (Fig. S2G, ESI†). Overall, these results demonstrated that wells could be implemented *in vitro* for the screening and quantification of molecules. In practice, these

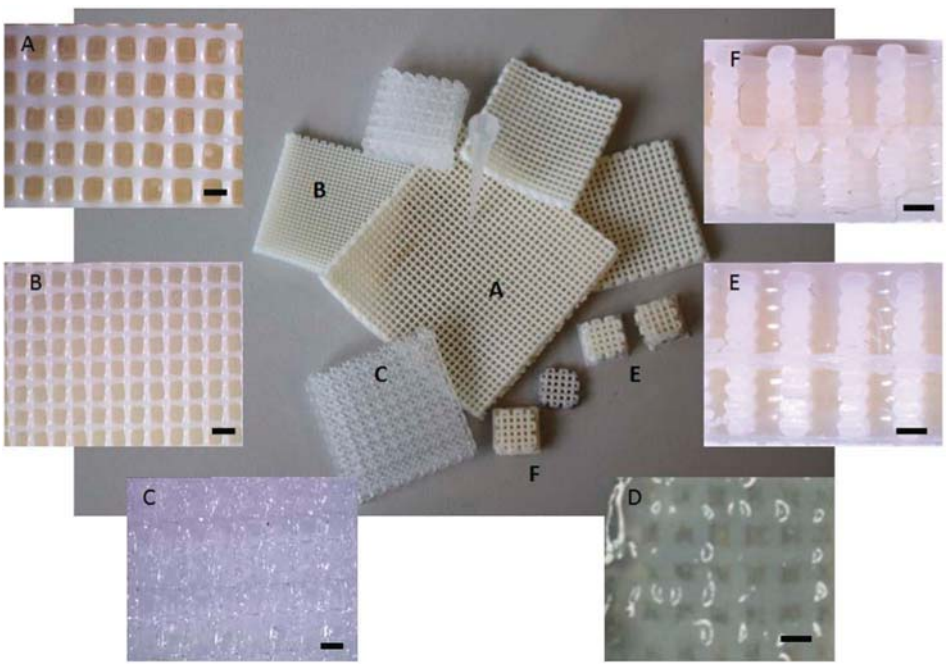

Fig. 1 Screening systems can be made of different sizes, materials and architectures. We were able to manufacture: 1024 wells in a 32 × 32 matrix made of PEOT–PBT of 300/55/45 composition (A); 100 wells in a 10 × 10 matrix made of PEOT–PBT of 1000/70/30 composition (B); 100 wells in a 10 × 10 matrix made of poly lactic acid (C); 100 wells in a 10 × 10 matrix made of alginate (in PBS) (D). The architecture of well systems could also be modified to create: a double matrix (top and bottom of a system) with a polymer layer in between (E); wells with a porous layer of material in the middle for potential co-culture studies (F). White arrow points to the pipette tip size that fits into a well. Scale bar: 1 mm.

 This journal is © The Royal Society of Chemistry 2013

Open Access Article. Published on 17 April 2013. Downloaded on 15/11/2014 00:35:09.

results showed that up to 9 wells per screening device could be consistently dispensed manually, and that the sensitivity of results was not compromised by the materials or the designs.

As a popular tissue regeneration cell source, hMSCs were selected for testing the cell culture compatibility of wells (Fig. 2) made of PEOT–PBT, a biocompatible copolymer already used in skin and musculoskeletal regenerative medicine applications.[8] The material was selected for its slow *in vivo* degradation,[17] low water uptake ($\sim$5%) and high tensile strength (up to 23 MPa).[18] In addition, attachment, proliferation and differentiation of chondrocytes[16] and hMSCs[19] can be tuned by varying the PEOT/PBT ratio of the copolymer chains. A 2D film of the material itself showed that when hMSCs were cultured on 300PEOT55PBT45 discs, cells organized in colony forming units (CFU's) (Fig. 2A), which resembled their known monolayer behavior on tissue culture plastic. In contrast, hMSCs cultured on rectangular wells formed 3D aggregates conditioned by the number of cells seeded (Fig. 2B). Remarkably, wells with the highest number of hMSCs contained 3D aggregates of random shapes whereas dilutions of hMSCs yielded wells with monolayer-type cultures. We determined that 3D aggregates augmented in size in a time-dependent manner due to the non-monolayer aggregation of hMSCs. To examine the effect of well-volume on hMSCs, the well size was varied in width and length and 1.2×10^4 hMSCs were seeded in three different types of wells (Fig. 2C–E), which effectively increases the cell concentration by decreasing the well volume instead of increasing the cell numbers. By adjusting the well size, an inverse correlation between hMSCs organization and well size was derived: hMSCs form 3D aggregates in the 0.45 μl well (Fig. 2C), while in the 1.8 and 4 μl wells (Fig. 2D and E) they organized into CFU's, leading to the conclusion that above 5×10^4 cells per μl of well hMSCs readily assemble in 3D aggregates. When low numbers of hMSCs are deposited in the well, these proliferate, increasing the cell concentration in time (Fig. 2F). From these data, we discovered that the 3D organization of hMSCs in the wells could be controlled through the well volume, cell number and culture time.

Based on molecular and cell culture results, we chose to fabricate PEOT–PBT screening systems with 9 wells and volumes of 1.8 μl per well. This meant that thirty six conditions could be housed in four subcutaneous sites in every immune-deficient mouse (Fig. S3, ESI†). The thirty six implanted conditions consisted of numbers of hMSCs, numbers of bovine primary chondrocytes (bPCs) and coculture ratios of hMSCs : bPCs that were screened for tissue regeneration markers (Table 1).

First, the systemic effect on the host tissue under the different conditions confined in the screening device was assessed in all twenty mice with markers for the cell nuclei, the cytoplasm of cells, keratin and collagen (Fig. 3). Interestingly, hair growth (Fig. 3A) was stimulated on the skin of nude mice

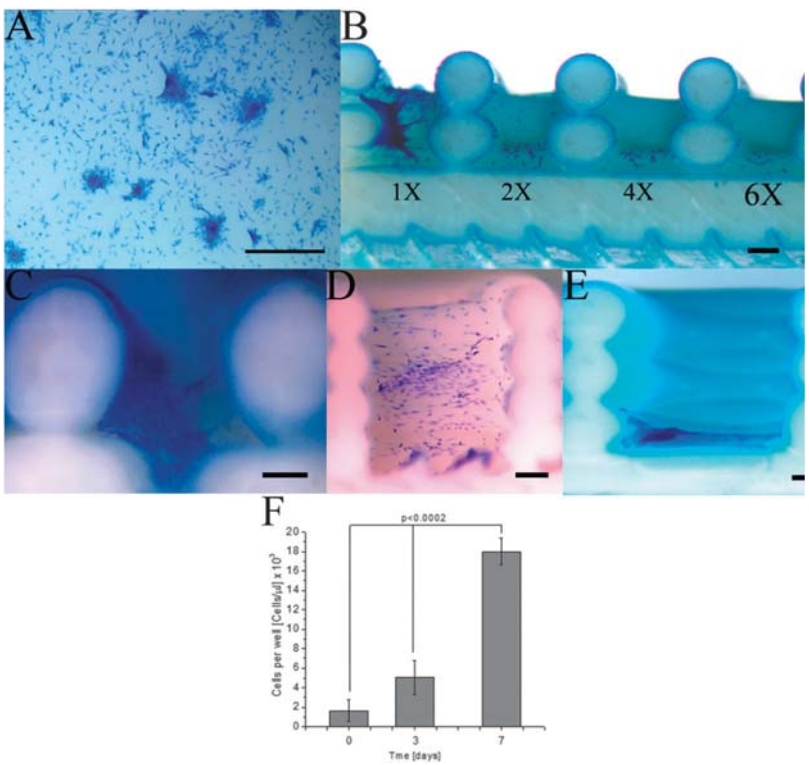

Fig. 2 Cell culture in the PEOT–PBT wells. 300 000 cells seeded on 2D PEOT–PBT colony forming units of methylene blue stained hMSCs. (A, top view), scale bar: 0.2 mm. When hMSC dilutions were tested in the PEOT–PBT wells, 25 000 hMSCs per μl produced 3D aggregates (B, cross section), scale bar: 0.5 mm. Varying the size of the wells and seeding 12 000 hMSCs in all well volumes showed that 0.45 μl wells induce 3D aggregate formation whereas 1.8 and 4 μl wells do not (C–E, cross section, scale bar: 0.2 mm). hMSC concentrations increase in time due to proliferation (F). One-way ANOVA followed by Tukey's *post hoc* test was used to evaluate statistical significance, where bars and error bars represent the mean cell number (n = 9 wells) and their standard deviation, respectively ($p < 0.01$).

Open Access Article. Published on 17 April 2013. Downloaded on 15/11/2014 00:35:09.

Table 1 Cell numbers for human mesenchymal stem cells (hMSCs), bovine primary chondrocytes (bPCs) and co-cultures screened with three replicates per cell condition and 9 control (empty) wells for a total of 36 conditions in each mouse

Dilution factor	hMSCs [cell #]	bPCs [cell #]	Co-culture ratios	hMSCs : bPCs [cell #]
1×	25 000	25 000	80 : 20	20 000 : 5000
2×	12 500	12 500	50 : 50	12 500 : 12 500
4×	6000	6000	20 : 80	5000 : 20 000

in wells containing hMSCs, indicating a systemic response to trophic factors.[20] Upon histopathological examination of tissue morphology in slides from all mice, there was no indication of cross-contamination of conditions or inflammatory responses (Fig. 3A). Instead, the first evident effect was the penetration/formation of tissue in the wells (Fig. 3B).

To evaluate the presence of tissue in the wells, we quantified the physical accumulation (tissue area/total well area) of tissue in each well for all mice (Fig. 4). Since the objective was to compare tissue penetration in all wells *vs.* the total well area, the analysed tissue area included implanted cells, host tissue and new ECM. Then we proceeded to identify patterns in time according to each condition. For example, the percent area of tissue in a well increased gradually with increasing numbers of hMSCs (Fig. 4A). Also bovine PCs exhibited an increase in tissue percent areas with increasing cell numbers on week 4 (Fig. 4B), but not on week 2. Despite seeding a maximum of 25 000 cells in all wells, co-cultures revealed growing tissue percent areas for wells containing increasing numbers of hMSCs (Fig. 4C). We analyzed the means of the percent area of tissue to determine whether there were significant differences between conditions. These led to variability of results between members of the same species when comparing all mice with each other. In wells with hMSCs, half of the mice displayed a significantly higher percent area of tissue between 6000 cells *vs.* control (no seeded cells, week 2), and 25 000, 12 000 cells *vs.* control (week 4) (Table S1, ESI†). Similarly, in wells with bPCs, half of the mice presented a significantly higher percent area of tissue between 25 000 cells *vs.* 12 000 cells (weeks 2 and 4), 12 000 cells *vs.* control (week 2) (Table S2, ESI†). Finally, in wells with co-cultures, 56% of the mice revealed significantly higher percent areas of tissue in the 20 000 hMSCs to 5000 bPCs (80 : 20) ratio *vs.* control (week 4) (Table S3, ESI†). Notably, there was no indication that the implantation site influenced the correlation between cell numbers and tissue percent areas according to the random distribution of conditions (Fig. S2, ESI†).

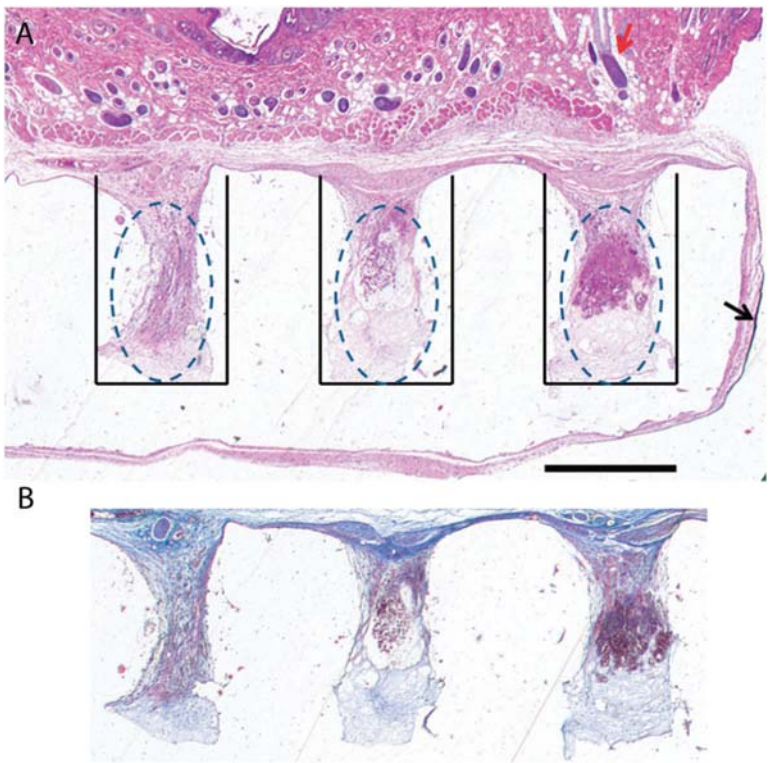

Fig. 3 *In vivo* screening is performed on histological sections showing three wells of a well system with the subcutaneous host tissue located above the wells. The representative staining of 80 screening devices is shown in this cross section of a 9-well device in 3 rows × 3 columns configuration. The red arrow points to hair growth on the skin of nude mice in wells containing hMSCs. The black arrow points to the area of the screening device stained with India ink to pinpoint the location of conditions (rows and columns) after histological processing. Sections of screening devices were stained with haematoxylin and counterstained with eosin showing the cytoplasm (red) and nuclei (dark blue), where the well is delineated with black lines and the material of the screening device appears to be white and enveloped by the host tissue (A). The dotted oval in (A) displays the area of interest for screening purposes, where implanted conditions interact with the host tissue. (B) The three wells are shown after Masson's tri-chrome staining: keratin (red), collagen (blue) and nuclei (dark brown) to evaluate the extracellular matrix in the wells. Notably, potential differences in the tissue penetration/formation per well were observed in each well. Scale bar: 1 mm.

 This journal is © The Royal Society of Chemistry 2013

Open Access Article. Published on 17 April 2013. Downloaded on 15/11/2014 00:35:09.

While *in vivo* cell proliferation was not investigated directly, the statistics (Tables S1 and S2, ESI†) did not support a significant correlation between increasing cell numbers and increasing percent areas of tissue (Fig. 4A and B). Since not higher than 50% of mice displayed a higher percent area of tissue under most conditions, it was concluded that increasing cell numbers were not sufficient to significantly increase the percent area of tissue in a well. Other effects such as the reverse trends in percent area of tissue for chondrocytes (week 2, Fig. 4B) were not significant. The most significant effect (in 56% of the mice) detected by quantifying the amount of tissue in a well was found for co-cultures, suggesting that co-cultures have the potential to induce higher percent areas of tissue when compared to the readings on empty wells (control), through ECM formation rather than cell numbers. Thus, it was concluded that the main contributor to the percent area of tissue in a well is the well itself probably due to tissue bulging[21] or penetration, which occurs spontaneously when host tissue is in contact with the well. In order of importance, tissue penetration was followed by tissue formation as the factor that increases the amount of tissue in a well as observed in 56% of the mice in wells with cocultures of four hMSCs to one bPC (80 : 20).

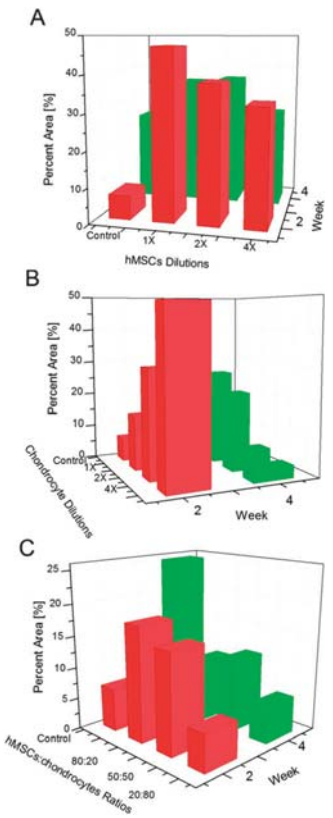

Fig. 4 Histological sections (>300 slides) contained tissue penetration/formation in wells which was evaluated through the percent area of tissue, defined as tissue area/well area × 100%. The means (n = 3 slides of a well) of the percent tissue area for each condition are graphically shown for two representative mice; one from week 2 and one from week 4. The percent tissue area increased as the number of cells in a well increased as depicted for hMSCs dilutions and control (empty well system) (A); bPCs dilutions and control (B). With a total of 25 000 cells per well in cocultures (C), the percent tissue area increased with higher ratios of hMSCs to bPCs.

Since hMSCs : bPCs cocultures have a known[22,23] cartilage regeneration potential, slides under all conditions were stained for proteoglycans (Fig. 5). It was found that when compared to other conditions (Fig. 5B–D), the co-culture containing the highest amount of hMSCs (80 : 20) was more strongly stained for proteoglycans (Fig. 5E). Upon histological grading[24] (Fig. 5F) of the quality of neo-cartilage, it was confirmed that all hMSCs : bPCs combinations produced a cartilage matrix. The 80 : 20 co-culture was the most promising condition tested in this screening showing *in vivo* cartilage regeneration as shown by the significantly higher cartilage (Bern) score on week 4.

To evaluate the results obtained for co-culture ratios using a conventional method (Fig. S4, ESI†), conditions were seeded in porous 3D scaffolds[16] and implanted subcutaneously in nude mice. These data also showed that proteoglycans increased in PEOT–PBT scaffolds containing cocultures with higher quantities of hMSCs (Fig. S4A, ESI†). The amount of GAG/DNA did not show a significant difference between groups (Fig. S4B, ESI†). However, the efficiency of proteoglycans production augmented with increasing ratios of hMSCs (Fig. S4B, ESI†). Sulphated-proteoglycans, collagen types I, II and IX confirmed that hyaline (healthy) cartilage-like tissue was more abundant in scaffolds with 80% and 90% hMSCs (Fig. S4C, ESI†).

Increasing the number of conditions that could be screened simultaneously in one animal improves the efficiency and speed at which therapies and treatments can be identified and translated into clinical practice. In fact, evaluating the same 36 *in vivo* conditions using conventional methods would have required 9 times the number of mice (Table 2).

Cross talk between wells and their physiological effect is condition-dependent. While wells *in vitro* can be independent of each other by adjusting the well volumes and the relative humidity, wells *in vivo* can interact with each other through soluble factors. The degree of interaction between wells will be dependent on molecule diffusion dynamics and time. In this study, ECM markers at 2 and 4 weeks did not indicate any cross talk between wells. However, this will be relative to the marker of interest. Even though cell therapy in conventional scaffold systems (50 mm^3) occurs in volumes over 25 times larger than well volumes (1.8 mm^3), both systems are consistent with the regions, where ECM production occurs, which is in the pores in scaffolds or inside the wells. This indicates that by reducing the volume of interest in the animal with wells, the extent of desired and undesired effects such as cross contamination is identifiable and controllable. As shown here, control can be achieved through randomization of implanted conditions, which ensures the discrimination of relevant biological responses, such as ECM production from irrelevant effects – for the purpose of this study – such as host tissue penetration in the wells.

Albeit 36 wells were investigated in nude mice as a proof of principle, the screening device has the potential to become a high throughput screening (HTS)[25,26] system where hundreds of wells can be contained in one animal with one well (1.8 μl) for every 1.4 mm of an implantation site. Depending on the size of the animal, these platforms can be tailored to fit the required dimensions of an implantation site, which defines the number

Open Access Article. Published on 17 April 2013. Downloaded on 15/11/2014 00:35:09.

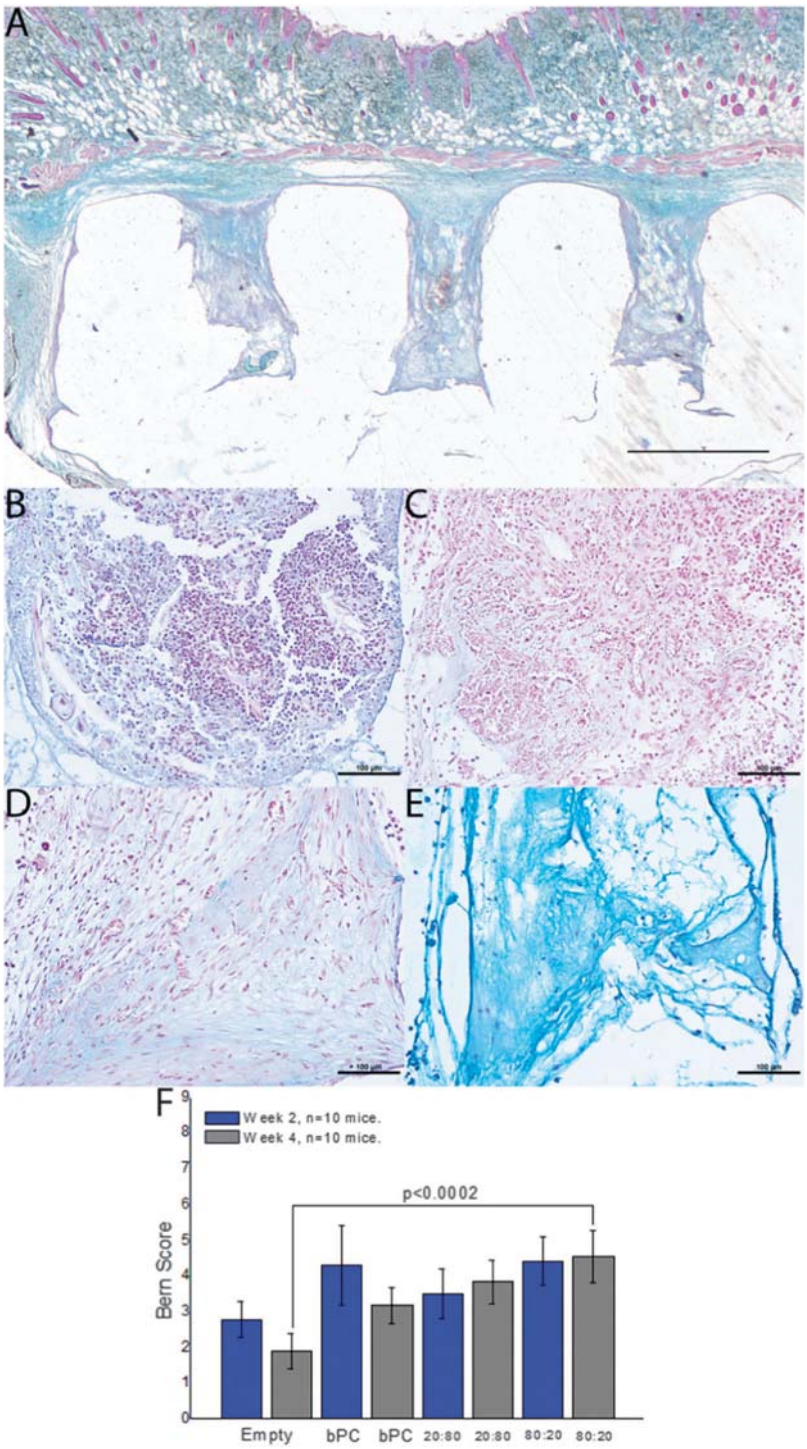

Fig. 5 Proteoglycan production was screened as a marker for cartilage formation. Glycosaminoglycans (GAG) (blue) and cytoplasm (red) seen in three wells of a screening device (A, scale bar: 1 mm). A representative slide of the control and three conditions expressing GAG are displayed: empty wells (B); 25 000 bPCs (C); co-culture of hMSCs : bPCs at a 20 : 80 ratio (D); co-culture of hMSCs : bPCs at a 80 : 20 ratio (E). Scale bars: 100 μm. Quantification of cartilage quality (F) from the screened conditions (mean Bern score, N = 10 mice) showed a significantly higher quality of cartilage for hMSCs : bPCs at a 80 : 20 ratio compared to control. Bern scores were analyzed with Kruskal–Wallis to evaluate significance followed by Bonferroni *post hoc* correction.

of conditions that can be implanted (Movie S1, ESI†). Thus, the larger the animal, the higher the number of conditions that can be investigated simultaneously. However, the seeding of macroscopic and large numbers (>100) of wells requires special equipment to control the microenvironment while dispensing conditions in all wells with reproducibility. Using the well system, the number of lives required to perform experiments in vertebrate animals is inversely proportional to the size of the

 This journal is © The Royal Society of Chemistry 2013

Open Access Article. Published on 17 April 2013. Downloaded on 15/11/2014 00:35:09.

Table 2 Projection of animals saved with implantable wells *vs.* a conventional method in a similar experimental set-up

Species	Experimental conditions	# Animals with conventional methods (n = 10 animals)	3D HTS well matrix	Size [mm]	Conditions per 3D HTS	Wells per animal	# Animals with 3D HTS	Animals saved
Mouse	36	90	3 × 3	4.2	9	36	10	80
Rats	576	1440	12 × 12	16.8	144	576	10	1430
Rabbits	1600	4000	20 × 20	28	400	1600	10	3990
Goats	4096	10 240	32 × 32	44.8	1024	4096	10	10 230

animal (Table 2), extending the possibility to assess multiple *in vivo* conditions. As shown here, standard histological methods offer an extensive wealth of data, yet methods that avoid histological processing[15,27,28] would be convenient to further optimize animal experiments, automatize the quantification and imaging, and improve the sensitivity and throughput of *in vivo* screening.

The efficiency of the developed animal-implantable well system not only lies in optimizing animal experiments, but also in bridging both *in vitro* and *in vivo* milieus. For example, the well system could be adapted to monitor biomechanics[29] and to elucidate gene regulatory networks[30,31] in live tissues. Multiple compounds such as nanoparticles, drugs or chemicals could be covalently or non-covalently attached to wells to increase the throughput of toxicity assessments and thereby drastically dwindle the use of vertebrate animal lives and costs in pharmaceutical, toxicological, chemical, and disease screening, while allowing for the first time to execute such screening in true three-dimensional tissues.

Experimental

Mesenchymal stem cell and chondrocyte isolation and culture

hMSCs and bPCs were isolated, cultured and cryopreserved as described before.[32] hMSCs were obtained from the acetabulum of five donors who were undergoing total hip replacement surgery and gave informed consent for bone marrow biopsy, approved by the medical ethical testing commission (METC) of the Medical Spectrum Twente in Enschede, The Netherlands. Gender and donor age were: Donor 1: female, 81 years. Donor 2: male, 65 years. Donor 3: female, 66 years. Donor 4: female, 66 years. Donors 1 to 3 were cultured in the wells *in vitro* and only Donor 3 was implanted in mice. Donor 4 was cultured in the porous scaffolds.

Well system fabrication

A Bioplotter device (Envisiontec GmbH, Germany), which is a *XYZ* plotter, was used to make the wells (European Patent Application: EP2404672A1) with a fabrication process adapted from that for scaffold fabrication.[16] To obtain well systems in a matrix form (columns × rows) (Fig. S1, ESI†), closed wells were made by depositing fibers on top of each other at a 90° angle to obtain rectangular wells, where the first layer deposited was always closed. The well dimensions were defined by increasing or decreasing fiber distances in the *XY* axis and by the height of the cubical model. This was reproducible with four materials with their respective parameters as shown in Table S1 (ESI†) and Fig. 1.

Different architecture designs were fabricated to maximize the number of wells and to create co-culture systems as shown in Fig. 1E and F. For the design in Fig. 1E, first and second layer strand distances were maintained as shown in Table S1 (ESI†) and a strand distance (0.5 mm) in the middle of the well height (at 2 mm) was introduced. The design in Fig. 1F did not have a closed first layer where a constant strand distance (Table S1, ESI†) was maintained until deposition of a closed layer in the middle of the well height (at 2 mm). Subsequently, layer deposition with a constant strand distance was resumed.

In vitro screening

Fluorescent microspheres (YG: λ = 441–486 nm) (Polyscience, Germany), rhodamine (Sigma-Aldrich) and FITC (Sigma-Aldrich) were diluted in PBS before seeding 1 μl of solution per well of photopolymerizable resin (Envisiontec, Germany) and poly lactic acid (Purac, The Netherlands) screening devices. Fluorescence was imaged in an automatic confocal light microscope (BD pathway, The Netherlands).

Well sterilization and conditioning for cell culture

Well systems were sterilized with 70% ethanol solution for 15 min, washed three times and incubated at room temperature for two hours with sterile PBS, and thereafter incubated in αMEM proliferation media overnight at 37 °C.

Well seeding

From a cell suspension of 5×10^6 cells per ml, hMSCs were centrifuged at 200 Relative Centrifugal Force (RCF) and re-suspended in 0.2 ml of medium. From this cell suspension, dilutions were prepared with a maximum of 2.5×10^4 cells in 1 μl volume seeded per well. Every condition (*i.e.* cell dilutions) was seeded in all the wells of a column. In a 3 × 3 well system, three replicates or three wells were seeded under the same condition. Seeded wells were incubated for 20 min at 37 °C in a humid atmosphere with 5% CO_2. Non-detached cells in a well were removed by washing with culture medium, then these were placed in a well of a 25-well plate (Nunc), and covered with the culture medium of hMSCs or bPCs and incubated at 37 °C.

In vitro cell culture

Cell numbers in wells were obtained using Cyquant DNA assay (Invitrogen). Cell numbers were calibrated for hMSCs by measuring the μg of DNA per cell of cell numbers from 1×10^3 to 3×10^5 cells against known DNA amounts. It was estimated that each hMSC contained 1.6 picograms of DNA, which made it possible to quantify cell numbers in wells.

Open Access Article. Published on 17 April 2013. Downloaded on 15/11/2014 00:35:09.

Co-culture preparation in wells

Human MSCs : bPCs were seeded in wells in αMEM proliferation media. Each of the three ratios (0.8 : 0.2, 0.5 : 0.5, and 0.2 : 0.8) was seeded in three wells of a 3 × 3 well system, which contained a maximum of 2.5×10^4 cells per well.

Implantations in immune-deficient mice

Nude mice studies were performed after consent from the ethical committee for animal studies (DEC-GDL Utrecht, The Netherlands). Six-week-old nude mice (Hdcpb : NMRI-nu Harlan, The Netherlands) were anaesthetized with 0.02 ml of a 3.5 : 3 : 1 mixture of ketamine (100 μg ml^{-1}) : xylazine (20 μg ml^{-1}) : atropine (0.5 μg ml^{-1}).

Four 3 × 3 well systems containing 36 conditions were subcutaneously implanted per mouse in the posterior-lateral side of the back and sutured. The 36 conditions implanted were triplicates of: three dilutions of hMSCs (25 000; 12 000; and 6000 cells); three dilutions of bPCs (25 000; 12 000; and 6000 cells); three hMSCs : bPCs ratios (0.8 : 0.2, 0.5 : 0.5, and 0.2 : 0.8) and empty wells with no cells. Conditions were randomized by dispensing them in different wells of screening devices and implanting devices in different pockets from one mouse to another (Fig. S3A, ESI†). After 2 weeks (n = 10) and 4 weeks (n = 10) mice were euthanized *via* CO_2 asphyxiation and screening systems were excised and processed for analysis.

Histology of screening devices

3 × 3 well systems were explanted, washed in PBS and fixed in 10% formalin at 4 °C overnight. After washing in PBS, wells were embedded in paraffin and cut into 5 μm sections using a microtome. Slides containing sections of 80 well systems were stained with haematoxylin and counterstained with eosin (H&E); alcian blue and counterstained with nuclear red; and Masson's tri-chrome. These samples were examined by GAH, LW, LMT and JL under direct supervision of CvB, LM and MK with a proven track record in histological evaluation of implants of more than 20 years.

Tissue quantification in wells

Slides showing 3 × 3 well system's rows were stained with H&E, Masson's trichrome and alcian blue and imaged using light microscopy. Image analysis was performed for the area containing each condition on ~350 representative slides, obtained from 80 screening devices and 3 representative sections per well. Images were processed by cutting the images of wells (Fig. S3B, ESI†) and converting them to a binary pixel image (Fig. S3C, ESI†) using ImageJ software (open source). Black and white pixels within an image of a well were quantified with the histogram function in ImageJ, where the mean (n = 3 slides) of the percent area of tissue was obtained for each explanted well system. Using a binary system, where black represented tissue and white represented lack of tissue in a well, it was possible to avoid thresholding biases and to quantify the pixels in the wells. In this manner, nuclei, cytoplasm and ECM (keratin, collagen and GAG) appeared as black pixels, and everything else as white pixels.

Bern score of cartilage in wells

The visual histological grading or the Bern score for the evaluation of neocartilage was performed by three independent observers as previously shown[24] for representative slides of conditions showing cartilage formation with alcian blue and counterstained with nuclear fast red. 170 images were printed, randomly organized and separately assessed by each independent observer to obtain a score for each condition in 20 mice.

Two-dimensional PEOT–PBT discs

Poly(ethylene oxide terephthalate)–poly(butylene terephthalate) (PEOT–PBT) was used to make 2D substrates, following an *a*PEOT*b*PBT*c* nomenclature, *a* is the molecular weight in g mol^{-1} of the starting PEG block for copolymerization, whereas *b* and *c* are the respective weight fractions of the PEOT and PBT blocks. Specifically, 300PEOT55PBT45 was used to manufacture 2D substrates by a hot-embossed compression molding technique, where two silicon wafers served as a support and defined the molded surface. A stainless steel mold with circular features through holes of 2.2 cm in diameter was placed in between the molds. Granules of 300PEOT55PBT45 were placed inside the mold to fill up the mold cavities upon polymer melting. Silicon supports were cleaned by immersion in piranha solution (3 : 1 concentrated H_2SO_4–33% aqueous H_2O_2) for 15 min. These were rinsed with water and dried in N_2. Then, they were functionalized with 1*H*,1*H*,2*H*,2*H*-perfluorodecyltrichlorosilane (ABCR). After that, these were deposited in the gas phase that served as an anti-adhesion layer to ease the polymer–support separation. For the hot embossing process, a hydraulic press equipped with a water cooling system and temperature control (Fortune, Holland, The Netherlands) was used. The 300PEOT55PBT45 was placed on top of the silicon support and in the aperture of the mold. Then, the system was heated up to a temperature of 180 °C and 10 bars were applied. After 5 minutes the system cooled down to 60 °C and the pressure was released. The mold and the supports were manually separated and the 2D disc released from the mold.

3D scaffold fabrication

The bioplotter device was also used to manufacture porous scaffolds. According to a previous study,[16] co-polymers were molten and deposited as successively layered fibers in a 0–90 pattern from a 250 μm nozzle onto a computer aided *x*/*y*/*z* table with a layer thickness of 0.15 mm and a fiber spacing of 0.6 mm. Cylindrical scaffolds (∅ 4 × 4 mm) with constant pore size and 100% interconnecting pore volume were cored and sterilized in isopropyl alcohol.

Seeding and co-culture of bovine PCs and human MSCs in scaffolds

Cylindrical scaffolds were extensively rinsed in phosphate buffered saline (PBS), incubated overnight in proliferation medium and blotted dry prior to seeding. Bovine primary chondrocytes were mixed with hMSCs, respectively, at a

 This journal is © The Royal Society of Chemistry 2013

Open Access Article. Published on 17 April 2013. Downloaded on 15/11/2014 00:35:09.

total of 3 million cells per scaffold, centrifuged at 300*g* for 5 minutes and re-suspended in 54 μl of medium containing 300 μg ml^{-1} fibronectin. Scaffolds were seeded statically with 3×10^6 cells per scaffold for 1 day before subcutaneous implantation in nude mice.

Implantation of bovine PCs and human MSCs in scaffolds

With 4 implants maximum per mouse, nine constructs of bovine PCs : hMSCs ($n = 9$) per experimental group (7 groups = 4 co-cultures plus 3 controls) were randomly implanted in 16 nude mice.

Histology and immunohistochemistry with scaffolds

Three constructs per donor were explanted, washed in PBS, fixated in formalin at 4 °C overnight. After washing in PBS, constructs were cut into 2 halves, one half was embedded in GMA and one half was embedded in Tissue-Tek for immunohistochemistry. GMA embedded 3D scaffolds were cut into 5 μm sections which were treated with safranin-O (red) to stain sulphated-proteoglycans, hematoxylin (dark blue) to mark the nuclei and with fast green (light blue) to label the cytoplasm. Scaffolds ($n = 3$) were embedded and immediately frozen at −80 °C in OCT compound (Tissue-Tek) for immunostaining. Sections were cut using a cryo-microtome to a thickness of 5 μm and fixated with acetone for 10 minutes, stained for collagen type-I (1 : 1000, Ab-1, Calbiochem), type-II (1 : 100, DSHB II-II6B3), and type-IX (1 : 100, DSHB D1-9). Blocking was achieved with 10% human serum and secondary antibody was goat anti-mouse (1 : 100, DAKO). Staining was visualized through incubation of slides in 3,3-diaminobenzidine (DAB)–solution (DAKO) for 10–20 minutes. These samples were examined by JH, MvdD and RS under direct supervision of CvB, LM and MK.

Statistical analysis

Normality of the data was analyzed by determining skewness being between −3 and 3 and showed normal distribution of the data in all groups. *In vitro* fluorescent data were analyzed for each condition as the mean ($n = 12$ wells) emission of wells with one-way Anova followed by Tukey's honestly significant difference criterion with statistical significance set at $p < 0.01$. Quantitative GAG and DNA data from scaffolds were analyzed for differences of the means ($n = 5$ scaffolds) with two-way Anova followed by Tukey's honestly significant difference criterion, where statistical significance was set at $p < 0.01$.

In vivo screening of conditions was organized in replicates with a multi-dimensional sample number, which was defined by $N = 10$ animals and $n = 3$ replicates per well for each condition in each animal. So that $n = 3$ replicates per condition per mouse and the total sample number per condition is $N \times n = 30$.

The mean ($n' = 3$ histological slides) of the percent area of tissue was analyzed for each screening device in each statistically independent mouse ($n = 3$ wells per condition in each animal) with one-way Anova followed by Tukey's honestly significant difference criterion where statistical significance was set at $p < 0.05$. So that for each mouse, there were $n' \times n = 9$ images of the same condition available for analysis.

Since Bern score data are non-parametric, it was not normally distributed data. To account for that, Bern scores of differences of means ($N = 10$ mice) for glycosaminoglycans in the well system were analyzed with Kruskal–Wallis with Bonferroni *post hoc* correction. Three independent observers assessed the Bern scores for each slide, where inter-observer reproducibility was evaluated with the hypothesis of a combined effect on Bern scores by both mean observers' score for a slide and a mean score for a condition causing a statistical significant difference set at $p < 0.05$.

Acknowledgements

The authors would like to acknowledge the financial support from the Dutch SenterNovem research grant number 15044112, Pre-seed grant number 93611002 of the Netherlands Genomics Initiative, and the TERM Smart Mix Program of the Netherlands Ministry of Economic Affairs and the Netherlands Ministry of Education, Culture and Science. The authors would like to thank Susan Nijhuis and Tessa Hering of the Laboratory of Pathology of the East Netherlands and Ewart de Bruijn for their histological expertise, and Dr Maryana Escalante for her input in the design of polymer discs.

References

1 K. Cheng, Y. Lai and W. S. Kisaalita, Three-dimensional polymer scaffolds for high throughput cell-based assay systems, *Biomaterials*, 2008, **29**, 2802–2812.
2 W. R. Inch, J. A. McCredie and R. M. Sutherland, Growth of nodular carcinomas in rodents compared with multi-cell spheroids in tissue culture, *Growth*, 1970, **34**, 271–282.
3 Comission, E. (ed Environment Directorate General) 19 (2007).
4 T. Hartung and C. Rovida, Chemical regulators have overreached, *Nature*, 2009, **460**, 1080–1081.
5 F. Khan, R. S. Tare, J. M. Kanczler, R. O. C. Oreffo and M. Bradley, Strategies for cell manipulation and skeletal tissue engineering using high-throughput polymer blend formulation and microarray techniques, *Biomaterials*, 2010, **31**, 2216–2228.
6 A. Peters, D. M. Brey and J. A. Burdick, High-throughput and combinatorial technologies for tissue engineering applications, *Tissue Eng., Part B*, 2009, **15**, 225–239.
7 P. B. Gupta, *et al.* Identification of selective inhibitors of cancer stem cells by high-throughput screening, *Cell*, 2009, **138**, 645–659.
8 L. Moroni, J. R. de Wijn and C. A. van Blitterswijk, Integrating novel technologies to fabricate smart scaffolds, *J. Biomater. Sci., Polym. Ed.*, 2008, **19**, 543–572.
9 D. R. Albrecht, V. L. Tsang, R. L. Sah and S. N. Bhatia, Photo- and electropatterning of hydrogel-encapsulated living cell arrays, *Lab Chip*, 2005, **5**, 111–118.
10 Y. Ibold, *et al.* Development of a high-throughput screening assay based on the 3-dimensional pannus model for rheumatoid arthritis, *J. Biomol. Screening*, 2007, **12**, 956–965.

Open Access Article. Published on 17 April 2013. Downloaded on 15/11/2014 00:35:09.

11 M. Schindler, *et al.* Living in three dimensions: 3D nanostructured environments for cell culture and regenerative medicine, *Cell Biochem. Biophys.*, 2006, **45**, 215–227.
12 C. M. Yen, C. C. Chan and S. J. Lin, High-throughput reconstitution of epithelial-mesenchymal interaction in folliculoid microtissues by biomaterial-facilitated self-assembly of dissociated heterotypic adult cells, *Biomaterials*, 2010, **31**, 4341–4352.
13 S. I. Montanez-Sauri, K. E. Sung, E. Berthier and D. J. Beebe, Enabling screening in 3D microenvironments: probing matrix and stromal effects on the morphology and proliferation of T47D breast carcinoma cells, *Integr. Biol*, 2013, **5**, 631–640.
14 G. A. Higuera, A. van Boxtel, C. A. van Blitterswijk and L. Moroni, The physics of tissue formation with mesenchymal stem cells, *Trends Biotechnol.*, 2012, **30**, 583–590.
15 K. M. Bratlie, *et al.* Rapid biocompatibility analysis of materials *via in vivo* fluorescence imaging of mouse models, *PLoS One*, 2010, **5**, e10032.
16 L. Moroni, J. A. Hendriks, R. Schotel, J. R. de Wijn and C. A. van Blitterswijk, Design of biphasic polymeric 3-dimensional fiber deposited scaffolds for cartilage tissue engineering applications, *Tissue Eng.*, 2007, **13**, 361–371.
17 A. A. Deschamps, *et al. In vivo* and *in vitro* degradation of poly(ether ester) block copolymers based on poly(ethylene glycol) and poly(butylene terephthalate), *Biomaterials*, 2004, **25**, 247–258.
18 A. A. Deschamps, *et al.* Design of segmented poly(ether ester) materials and structures for the tissue engineering of bone, *J. Controlled Release*, 2002, **78**, 175–186.
19 A. Nandakumar, *et al.* Combining technologies to create bioactive hybrid scaffolds for bone tissue engineering, *Biomatter*, 2013, **3**, e23705.
20 A. I. Caplan and J. E. Dennis, Mesenchymal stem cells as trophic mediators, *J. Cell. Biochem.*, 2006, **98**, 1076–1084.
21 G. Lemon, *et al.* Growth of the chorioallantoic membrane into a rapid-prototyped model pore system: experiments and mathematical model, *Biomech. Model. Mechanobiol.*, 2011, **10**, 539–558.
22 J. Fischer, A. Dickhut, M. Rickert and W. Richter, Human articular chondrocytes secrete parathyroid hormone-related protein and inhibit hypertrophy of mesenchymal stem cells in coculture during chondrogenesis, *Arthritis Rheum.*, 2010, **62**, 2696–2706.
23 X. Liu, *et al. In vivo* ectopic chondrogenesis of BMSCs directed by mature chondrocytes, *Biomaterials*, 2010, **31**, 9406–9414.
24 S. P. Grogan, *et al.* Visual histological grading system for the evaluation of *in vitro*-generated neocartilage, *Tissue Eng.*, 2006, **12**, 2141–2149.
25 L. A. Kunz-Schughart, J. P. Freyer, F. Hofstaedter and R. Ebner, The use of 3-D cultures for high-throughput screening: the multicellular spheroid model, *J. Biomol. Screening*, 2004, **9**, 273–285.
26 E. Stokstad, Putting chemicals on a path to better risk assessment, *Science*, 2009, **325**, 694–695.
27 R. Bhargava, D. C. Fernandez, S. M. Hewitt and I. W. Levin, High throughput assessment of cells and tissues: Bayesian classification of spectral metrics from infrared vibrational spectroscopic imaging data, *Biochim. Biophys. Acta*, 2006, **1758**, 830–845.
28 S. Judex, *et al.* Quantification of adiposity in small rodents using micro-CT, *Methods*, 2010, **50**, 14–19.
29 R. La and M. F. Arnsdorf, Multidimensional atomic force microscopy for drug discovery: a versatile tool for defining targets, designing therapeutics and monitoring their efficacy, *Life Sci.*, 2010, **86**, 545–562.
30 D. D. Licatalosi, *et al.* HITS-CLIP yields genome-wide insights into brain alternative RNA processing, *Nature*, 2008, **456**, U464–U422.
31 T. Whitington, A. C. Perkins and T. L. Bailey, High-throughput chromatin information enables accurate tissue-specific prediction of transcription factor binding sites, *Nucleic Acids Res.*, 2009, **37**, 14–25.
32 L. Wu, *et al.* Trophic effects of mesenchymal stem cells increase chondrocyte proliferation and matrix formation, *Tissue Eng., Part A*, 2011, **17**, 1425–1436.

 This journal is © The Royal Society of Chemistry 2013